Journal of Low Temperature Physics (2020) 200:336–341
https://doi.org/10.1007/s10909-020-02475-6

Fabrication of Bismuth Absorber Arrays for NTD-Ge Hard X-ray Microcalorimeters

S. Ferruggia Bonura[1,2] · D. Gulli[2] · M. Barbera[1,2] · A. Collura[2] · D. Spoto[3,2] · P. Vassallo[4] · S. Varisco[2] · M. Santamaria[4] · F. Di Franco[4] · A. Zaffora[4] · L. Botta[4] · U. Lo Cicero[1,2]

Received: 20 August 2019 / Accepted: 15 May 2020 / Published online: 22 May 2020

Abstract

The high-spectral-resolution detection of hard X-rays (E > 20 keV) is a challenging and nearly unexplored area in space astrophysics. Traditionally hard X-ray detectors present moderate spectral resolutions, although few tens of eV one could open new frontiers in the study of nuclear processes and high-temperature plasma dynamics in energetic processes. This can be achieved by using cryogenic microcalorimeters. Within a research activity aimed at developing arrays of neutron transmutation-doped germanium (NTD-Ge) microcalorimeters for the high-spectral-resolution detection (about 50 eV@60 keV) of hard X-rays (20 keV < E < 100 keV), we developed an electroplating process to fabricate high-thickness (> 60 μm) bismuth absorber arrays. The adopted technological process and the study of related process parameters are discussed; preliminary results on produced arrays are given.

Keywords Hard X-rays · Low-temperature detectors · NTD-Ge microcalorimeters · Bismuth absorbers · Bismuth electroplating

✉ S. Ferruggia Bonura
salvatore.ferruggiabonura@unipa.it

[1] Dipartimento di Fisica e Chimica - Emilio Segrè, Università degli Studi di Palermo, Via Archirafi 36, 90123 Palermo, Italy

[2] Istituto Nazionale di Astrofisica, Osservatorio Astronomico di Palermo, Piazza del Parlamento 1, 90134 Palermo, Italy

[3] Agenzia Spaziale Italiana (ASI) – Via del Politecnico, 00133 Rome, Italy

[4] Università degli Studi di Palermo, Dipartimento di Ingegneria, Viale delle Scienze, 90128 Palermo, Italy

1 Introduction

Electromagnetic radiation emissions observed in the X-ray band (0.1–100 keV) by nearly all types of stars across the Hertzsprung–Russell diagram, black holes, supernova remnants and galaxy clusters allow to acquire a quite solid understanding of these object physics [1]; elemental composition, density, temperature and other characteristics can be evaluated by analyzing grabbed spectra mainly in the soft X-ray band (< 10 keV).

Many efforts have been already put to observe the universe in the hard (10–100 keV) X-ray band, e.g., NASA InFOCμS [2] and ESA INTEGRAL [3] missions, but traditionally used CdTe/CdZnTe semiconductor-based hard X-ray detectors present moderate spectral resolution (several hundred eV @ 60 keV), while a resolution of few tens of eV at such energies could open new frontiers in the study of nuclear processes and high-temperature plasma dynamics in energetic processes.

Cryogenic microcalorimeters can satisfy such requirement. Both NTD-Ge [4] detectors and transition edge sensors (TES) [5] already reached appealing characteristics related to energy and space resolution, count rate and quantum efficiency; presently, such devices are currently investigated for the detection of soft X-rays from astrophysical sources (e.g., the TES microcalorimeters in the Athena X-ray Integral Field Unit instrument [6]).

In the past, the authors studied a technology to fabricate NTD-Ge arrays using planar technologies [7]. Recently, we have started a feasibility study for a balloon-borne experiment (MISTER-X), aimed to observe the solar corona in the hard X-ray band (20–100 keV) at high spectral resolution (about 50 eV @ 60 keV) by using NTD-Ge microcalorimeters to gain more detailed information on our star physics.

The aim of this research is to design and fabricate bismuth absorbers for NTD-Ge microcalorimeter arrays. We already developed a process to deposit Sn absorbers [8], a material that is not, however, suitable for hard X-rays absorption. Bismuth is a good material for hard X-ray absorber fabrication, due to: efficient X-ray absorption; very low heat capacity; high growth thicknesses, giving high quantum efficiencies also at E > 50 keV; simple growth technology (electroplating); and moderate cost.

High-thickness bismuth layers were already deposited on glass substrates by electroplating, and a specific process was developed for this purpose [9].

2 Array Patterning and Substrate Preparation

Different 4×4 array patterns were designed, each of them with 400 μm pitch, whose different pad sizes and gaps range in the fields 200×200 μm^2 to 375×375 μm^2 and 200 μm to 25 μm, respectively; they were designed to study the feasibility of unguided growth, the uniformity of the process and the bismuth lateral growth to optimize detector quantum efficiencies related to array fill factors. All patterns were collected in a single layout (Fig. 1).

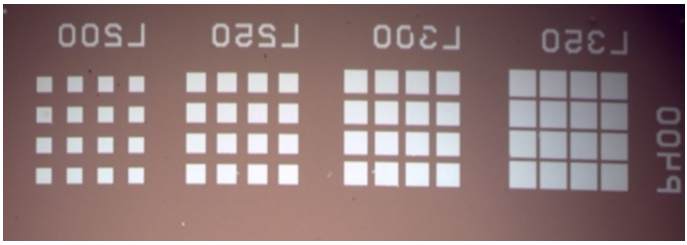

Fig. 1 Mask layout for microlithographic absorber array patterning (Color figure online)

To transfer such layout on electroplating substrates, a $3'' \times 3''$ iron dioxide-coated glass microlithographic mask was patterned, using this procedure: degrease in trichloroethylene (TCE), rinse in acetone, final rinse with absolute ethanol; MA-P1225 photoresist spin coating: 60 s @ 4000 rpm; soft baking in oven 5 min @ $T = 90$ °C; high-resolution direct laser exposure (at Dipartimento di Ingegneria of the Università di Palermo-UNIPa); photoresist development with ma-D 331, 1 min at room temperature, and rinse in deionized water; and iron dioxide wet etch with an iron (II) chloride-based solution. The optical inspection of the layout evidenced the correct opening of all designed features. A section of the fabricated mask optical microscope photograph is reported in Fig. 1.

Samples were prepared at the Microtechnology laboratory of X-ray Astronomy Calibration and Testing (XACT) facility, Osservatorio Astronomico di Palermo–Istituto Nazionale di Astrofisica (INAF-OAPA), in a class 10,000 clean room. Glass slices, whose dimensions were $25 \times 12.5 \times 1$ mm^3, were at first optical grade cleaned by the above-described multi-step procedure. Cleaned samples were then coated with 20 nm Ti and 20 nm Au by a Varian VT114A electron beam evaporation system.

The following microlithographic process to transfer array patterns on samples was used. Samples were firstly coated with a ~ 3-μm-thick MA-P1225 photoresist layer by a Kemat Technology KW 4A spin coater at 2000 rpm for 60 s, and a visual inspection allowed to state the lack of pinholes; then, they were soft-baked in oven at 90 °C for 10 min. Then photoresist exposure by a Suss MA6 mask aligner in hard contact mode at 10 mW/cm^2 UV intensity for 30 s and related development by ma-D 331 developer at room temperature for 60 s were performed; finally, samples were rinsed with deionized water.

3 Bismuth Electrodeposition on Patterned Substrates

Bismuth pixel arrays were grown by the electroplating technique on the patterned substrates. The deployed process was already developed by the authors at the Applied Electrochemistry Lab of the Dipartimento di Ingegneria of UNIPa, and related details are reported in [9]; the bismuth deposition was controlled by a Parstat 2263 potentiostat, in a three-electrode configuration, in which the gold-coated

sample was the working electrode, a dimensionally stable anode was the counter electrode, and an Ag/AgCl with KCl 3 M electrode was the reference electrode.

The solution composition is reported in [9]; its pH = 0.10, measured by a Hanna laboratory pH meter; the room temperature bath was moderately magnetically stirred during the deposition, to increase the layer uniformity.

Process parameters (applied electric potential, circulating charge, bath composition, fluid dynamic conditions and bath temperature) have to be careful controlled as the properties of the electrodeposited layers such as thickness, composition and morphology are strictly dependent on them. Deposition voltages were set between $E_s = -$ 50 mV and $E_s = -$ 100 mV, as it allowed to obtain good bismuth layer morphologies.

At first, a test pattern, containing several different shapes, dimensions and gap pads, was designed and fabricated, to study bismuth growth in tridimensional structures; this study was intended to evaluate both shape and area stability during accretion of bismuth, to estimate the bismuth layer morphology for different thicknesses and to estimate the growth uniformity of single structures related to the overall pattern. Scanning electron microscope (SEM) observations on growth structures, performed at the Dipartimento di Ingegneria of UNIPa, evidenced that their surface areas increase with the related heights, and the stirring speed influences their shapes.

Successively several bismuth arrays were grown on the samples presented in Sect. 2, varying the electroplating voltage (−50 mV or −100 mV), deposition time (1 to 3 h) and stirring rate (150 rpm or 300 rpm).

Examples of the obtained results are shown in Fig. 2, in which three different 4×4 pixel arrays, about 360×360 μm^2 each one with about 40 μm gaps in (c), 10 to 40 μm in (a) and (b), are depicted. The fill factor is about 81% in (c), slightly more in b). Deposition parameters for these arrays were: (a) $E_s = -50$ mV, accretion time 1 h, stirring speed 150 rpm; (b) −50 mV, 3 h, 300 rpm; and (c) −100 mV, 1 h, 300 rpm. Bismuth thicknesses are 42 μm, 55 μm and 15 μm, respectively. By studying obtained structures, a lot of information was gained. Firstly, electroplating potential influences bismuth morphology: At $E_s = -$ 50 mV (corresponding to lower

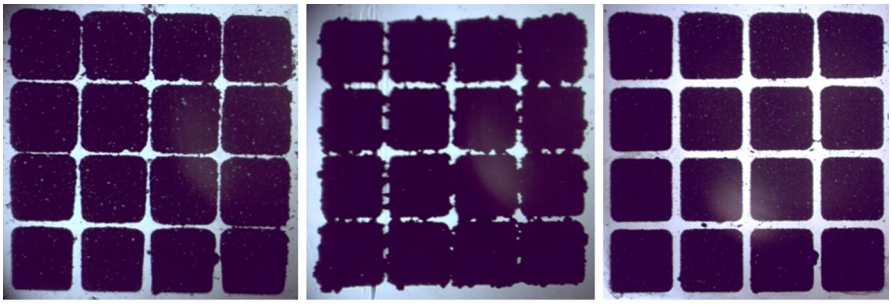

Fig. 2 Optical microscopy of 4×4 bismuth arrays with 360×360 μm^2 pixel size and 40 μm gaps; (**a**) −50 mV, 1 h, 150 rpm, 42 μm thickness; (**b**) −50 mV, 3 h, 300 rpm, 55 μm thickness; (**c**) −100 mV, 1 h, 300 rpm, 15 μm thickness (Color figure online)

cathodic overvoltage for Bi electrodeposition process), it produces smoother surfaces with respect to more negative potential (i.e., − 100 mV). About 10% enlargement on each side was estimated for each bismuth pixel with respect to the mask layout; this is due to the lateral deposition during the metal accretion. This enlargement strongly depends on process time. The longer is the deposition time (i.e., the thicker is the layer), the higher is the possibility of a lateral growth due to the influence of ohmic drop inside the Bi layer and the consequent impact on the current lines distribution (see Fig. 2a, b, c).

The stirring speed seems to influence also the pixel growth; it can be well seen by comparing Fig. 2a, c, related to processes developed at 150 rpm and 300 rpm, respectively. In (a), pixels are almost square with right, slightly rounded, angles, but there is less uniformity in lateral growth; in (c), upper row pixels (in the photograph) show increased shape deformation near the upper left corner probably due to the bath stirring. In (a) and (b), inhomogeneous gaps are produced by the incomplete control of the lateral growth.

The morphology of the deposited layers was studied by scanning electron microscopy. Figure 3a, b shows the SEM micrographs of bismuth layers grown at − 50 mV and − 100 mV for 30 min under stirred condition (300 rpm). The surface morphologies depend on the electrodeposition potential [10]. Indeed, the layer grown at − 50 mV is smoother with respect to that grown at − 100 mV, suggesting that at higher cathodic overvoltage ($E = -100$ mV) the faster growth induces the formation of a less uniform surface. Further details about the influence of electrodeposition parameters (pH, electrolytic bath composition, temperature, hydrodynamic conditions, etc.) on the morphology of Bi layers will be presented in a forthcoming paper.

4 Conclusions

In this work, an approach to fabricate bismuth absorbers for NTD-Ge microcalorimeter arrays was explored. Custom array patterns were designed and recorded on a suitable microlithographic mask. Preliminary tests on bismuth 3D structure growth were performed, by deploying an electroplating process for thick bismuth layer

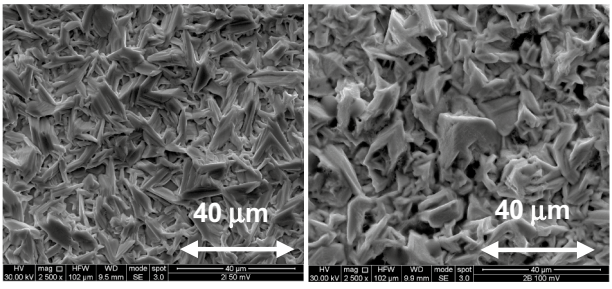

Fig. 3 SEM morphologies of two Bi samples: (**a**) − 50 mV; (**b**) − 100 mV

deposition previously developed, to acquire information on the material accretion process.

Optical microscopy observations on growth test samples evidenced that structure surface areas increase with related heights, and the stirring speed may influence their geometrical shapes.

Several 4×4 bismuth pixel arrays were grown with different parameters.

By evaluating the pixel size increase with their height, the array fill factor can be optimized. Thick depositions can produce small lateral dendrite formation, and this is to be avoided as it can provoke short heat circuits among pixels. A method is using a much thicker photoresist layer for array patterning to guide bismuth growth, and it will be applied in future experiments. The role of stirring has to be furtherly investigated, to confirm its influence and to avoid pixel shape deformation during growth.

Acknowledgments This research has been supported by Istituto Nazionale di Astrofisica (INAF) and Agenzia Spaziale Italiana (ASI), in the framework of the MISTER-X balloon-borne experiment preliminary activities. The authors thank prof. Giuseppe Lullo of Dipartimento di Ingegneria—Università di Palermo—for relevant support in patterning the microlithographic mask.

References

1. M.S. Longair, *High energy astrophysics*, 3rd edn. (Cambridge University Press, Cambridge, 2011). ISBN 978-0-521-75618-1
2. https://asd.gsfc.nasa.gov/archive/infocus/
3. http://sci.esa.int/integral
4. E. Silver et al., Proc. SPIE **4140**, 397–401 (2000). https://doi.org/10.1117/12.409135
5. A.R. Miniussi, J.S. Adams, S.R. Bandler et al., J. Low Temp. Phys. **193**, 337 (2018). https://doi.org/10.1007/s10909-018-1974-4
6. F. Pajot et al., J. Low Temp. Phys. **193**, 901 (2018). https://doi.org/10.1007/s10909-018-1904-5
7. U. Lo Cicero et al., Proc. IEEE Nucl. Science Symp. Conf. Record, NSS'08, 1789-1792 (2008), https://doi.org/10.1109/nssmic.2008.4774739
8. U. Lo Cicero et al., Proc. AIP Conf., 1185, 112-114 (2009), https://doi.org/10.1063/1.3292295
9. S. Ferruggia Bonura et al., Proc. SPIE 10709 (2018), https://doi.org/10.1117/12.2314195
10. I. Svancara et al., Electroanalysis **17**, 103 (2005). https://doi.org/10.1002/elan.200403061